Surface modification of cellulose nanofiber using silane coupling agent for poly(methyl methacrylate) reinforcement

Hiroyuki Kono*
Division of Applied Chemistry and Biochemistry, National Institute of Technology, Tomakomai College
Fax: 81-144-67-8036, e-mail: kono@tomakomai-ct.ac.jp
*Nishikioka 443, Tomakomai, Hokkaido 059 1275, Japan

The eco-friendly fiber-reinforced composite resins is one of the important objectives from an environmental perspective. Nanofibrillated bacterial cellulose (NFBC), with extremely long high-aspect-ratio fibers, is a filler material with high potential for use in such composite resins. Herein, chemically modifying the surfaces of NFBC fibers by coupling with (3-aminopropyl)trimethoxy-silane (APTMS) was investigated and nanocomposite materials using the prepared surface-modified NFBC was fabricated in this study. The product prepared by the one-pot reaction of APTMS with NFBC dispersed in aqueous solution retained the nanofibril structure as the intact NFBC. The degree of molar substitution as well as the silicon states on the surface depended on the feed amount of APTMS in the preparation. Highly transparent poly(methyl methacrylate) (PMMA)-based nanocomposites could be prepared by solvent casting method. In addition, tensile strength of the nanocomposite was more than twice that of neat PMMA when 1 wt% of the modified NFBC was added. Therefore, it is expected that the modified NFBC is a reinforcing nanofiber material that imparts excellent physical properties to fiber-reinforced resins.
Key words: Cellulose nanofiber, bacterial cellulose. Fiber-reinforced resins, nanocomposite.

1. INTRODUCTION

With increase of environmental pollution and the energy crisis, lightweight structures designed using nanofiber-containing polymer composite materials have attracted significant levels of attention from industry. Among various natural fibers, cellulose nanofiber (CNF) is the most promising one for the preparation of fiber-reinforced composites because of its natural abundance and the accumulated wealth of knowledge on their characteristics. Various methods for the preparation of CNFs have been investigated through mechanical and chemical treatments of lignocelluloses [1]. The diameters of these CNFs range from several nanometers to 100 nm, with lengths of up to several micrometers. Another source of CNF is bacterial cellulose (BC), which is produced by the gram-negative obligate aerobe, *Gluconacetobacter*. The BC is obtained as a gel-like membrane in static culture, and is an almost pure cellulose. The pellicle has a structure in which cellulose microfibrils with a diameter of approximately 100 nm are entwined three-dimensionally. According to recent reports [2,3], nano-fibrillated bacterial cellulose (NFBC) with a diameter of approximately 20–40 nm could be obtained by culturing a cellulose-producing bacterium with aerobic agitation in an aqueous medium, and the so-obtained NFBC can be uniformly dispersed in water, similar to other CNFs. The advantage of NFBC is that it could be directly obtained by the "bottom-up process" without mechanical and/or chemical disintegration of the thick cellulose fibers. Therefore, the NFBC has very long fibers (>15 μm), that is, it has a very high aspect ratio as well as other superior features such as homogeneity, dispersibility, and large surface area. The superiority of these characteristics of NFBC renders it suitably for various applications such as fiber-reinforced composites [4,5].

In order to disperse the NFBC in organic solvents and polymer matrices, a surface modification treatment of is required to render them compatible with these solvents and polymer matrices. Among various method for the surface modification of cellulose, silane coupling reaction is expected to be suitable for the cellulose nanofibers. Silane coupling agent play an important role in the preparation of composite from organic polymers and inorganic fillers such as glass, minerals, and metals [6]. The general structure of silane coupling agents are $(RO)_3$-Si-X, where X is an organofunctional groups, and RO is a hydrolysable group such as an alkoxy group. The surface modification of cellulose by silane-coupling agent begins with the solvolysis of these alkoxy groups by a catalyst (either an acid or a base), before it reacts with the cellulose surface. After the solvolysis, the formed silanol groups react with the hydroxyl groups of cellulose, which results in the modification of the cellulose surface (Fig. 1) [4,5].

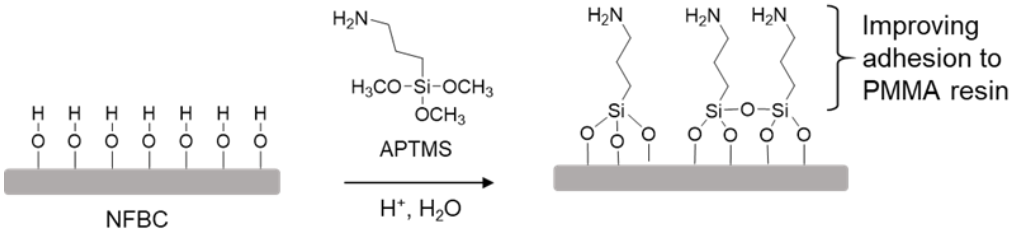

Fig. 1. Surface modification of NFBC for poly(methyl methacrylate) reinforcement

In this study, we demonstrated demonstrate the potential of NFBC for the reinforcement of polymer composite materials. PMMA and (3-aminopropyl)trimethoxysilane (APTMS) were selected as the polymer matrix for NFBC and the silane coupling agent, respectively. A series of APTMS-modified nanofibrillated bacterial cellulose surfaces (APC) were prepared with various NFBC:APTMS ratios (Fig. 1). The optimal surface-modification conditions were determined by characterizing APC samples by FTIR, solid-state NMR, XRD, and TG/DTA analyses. In addition, nanocomposites were prepared by solvent casting of PMMA with APC, and the properties of the composite was experimentally evaluated.

2. EXPERIMENTAL

2.1 Materials

The NFBC suspension in water was prepared according to a previously reported method [2]. PMMA (Mw: 120,000) was purchased from Sigma-Aldrich (USA). Other chemicals were of high purity, and all solutions were prepared with deionized water.

2.2 APC preparation

2 wt % NFBC suspension (600 mL, 6 g of cellulose in dry state) was adjusted the pH to 4, and APTMS (3.3 mL, 14 mmol) was added to the NFBC suspension. The silane coupling reaction was carried out with stirring for 4 h at 25 °C. The resulting product was washed with water, collected by centrifugation, and then freeze-dried to obtain APC 1. APCs 2–4 were prepared in a similar manner, but with different amounts of APTMS, namely 6.6 mL (28 mmol), 9.9 mL (42 mmol), and 17.5 mL (75 mmol), respectively [5].

2.3 Structurally characterizing the APCs

Solid-state NMR experiments were performed at 25 °C on a Bruker AVIII500 spectrometer equipped with a 4-mm magic angle spinning (MAS) probe. XRD was performed at 25 °C on a Bruker D8 Advance diffractometer equipped with a CuKα (λ = 0.1542 nm). XRD data were collected at 40 kV and 50 mA.

2.4 Morphological observation

SEM observation were carried out using a Jeol JSM-7500F electron microscope. The specimen was coated with Pt and observed at 7 kV. The fibril-width was determined using *ImageJ* Ver. 1.51w13 software, with average widths calculated from 100 randomly selected points on the fibers in the SEM images.

2.5 Nanocomposite preparation and tensile test

APC 2 was added to the PMMA (6.0 g) dissolved in THF (60 mL) and then completely dispersed using homogenizer at 15,000 rpm for 5 min. Each suspension (30 mL) was cast onto a Teflon petri dish and the solvent was evaporated at 70 °C for 12 h to produce 0.5, 1.0, and 2.0 wt% APC/PMMA nanocomposite [5].

Tensile testing was performed using strip specimens (5 cm × 1 cm) cut from cast films with a press-punch apparatus. A model AG-X plus 10kNX load frame with a 500-N load cell (Shimadzu) was used in these experiments. The specimens were in-tension loaded at a crosshead speed of 3.0 mm/min.

3. RESULTS AND DISCUSSION

3.1 Structural characterization of APC

Fig. 2 shows the solid-state ^{13}C and ^{29}Si NMR spectra of APC 4 and NFBC with the results of the resonance assignments. In addition to signals for the anhydroglucose units of cellulose, the ^{13}C NMR spectra of the APC samples show three carbons 7, 8, and 9 due to the aminopropyl groups at 43, 22, and 11

ppm. Integration of these resonances relative to the C1 resonance enabled the degree of molar substitution (MS), i.e., the number of APTMS molecules that had reacted per anhydroglucose residue (AGU). As a result, the MS values of APCs 1–4 could be determined to be 0.07, 0.24, 0.26, and 0.27, respectively, indicating that the MS value increases with increasing amount of added APTMS, especially in going from APC 1 to 3, but becomes saturated at APC 4.

In the ^{29}Si NMR spectra of APC (Fig. 2, right), four silicon states coupled to cellulose, namely, a monomer (T0) through singly (T1), doubly (T2), and fully (T3) condensed silicon atoms appear at –41, –52, –58, and –65 ppm, respectively. Line-fitting analyses of these ^{29}Si NMR spectra enabled the ratios of the four silicone states in each sample to be determined. The T0–T3 state populations depended on the sample; the proportions of T0, T1, and T2 were determined to be 34%, 65%, and 1% for APC 1; 18%, 77%, and 4% for APC 2; 15%, 79%, and 6% for APC 3; and 0%, 81%, and 17% for APC 4, respectively, with the T3 state only observed for APC 4, albeit a very small population (2%). These results indicate that the APTMS molecules tend condense at high concentrations during the preparation of the APC samples [4,5].

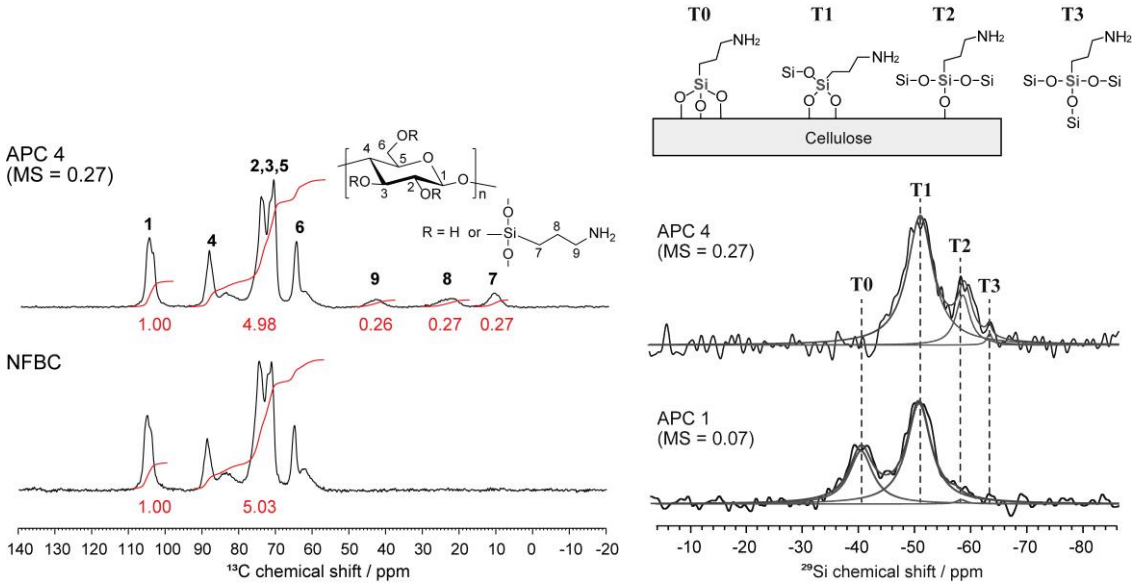

Fig. 2. Solid-state ^{13}C (left) and ^{29}Si (right) NMR spectra of NFBC and APC 4 [5]. The integral value of carbon 7 relative to that of the C1 resonance corresponds to MS of APC samples (left). Schematically illustrating the monomer (T0), and singly (T1), doubly (T2), and fully (T3) condensed silicon atoms following the reaction of APTMS with the cellulose surface (right).

3.2 Morphology of APC and NFBC

Fine fiber structures are clearly detected in the SEM images of NFBC and APCs 1–4 (Fig. 3). Average widths APC 1–4 fibrils are 27.6 nm, 29.4 nm, 29.7, and 30.2 nm, respectively, while that of the NFBC is 25.8 nm. The observation that the average fiber width of the APC samples gradually increases with increasing sample MS indicates that the silane coupling reaction involving proceeded on the NFBC surface to form the polysiloxiane domain.

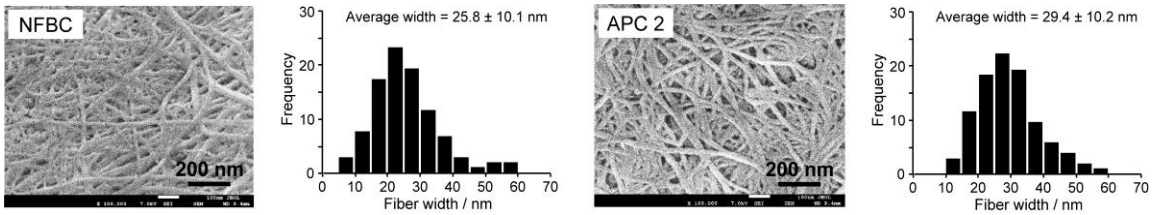

Fig. 3. SEM photograohs and fibril width distributions (n = 100) of the NFBC and APC 2 [5].

3.3 Preparation and characterization of the nanocomposites

Since the APC 2–4 has almost same MS and exhibit almost identical dispersion properties in THF, it was considered that the surface of these samples was completely coated with a polysiloxane domain. Therefore, APC 2 was selected and used as a filler for preparing nanocomposites with PMMA.

Fig. 4 shows PMMA and APC/PMMA nanocomposites prepared by blending 0.5, 1.0, and 2.0 wt% APC 2. The nanocomposites were almost transparent with no fiber aggregation visually detected. Fig. 5 shows the transparencies of the nanocomposites and PMMA in the visible region. PMMA was uniformly transparent (94%), while the transparencies of the nanocomposites depended on the wavelength. In addition, the transparency of the nanocomposite decreased as a function of APC 2 concentration, indicating that the decrease in transparency is caused by overlapping APC 2 fibrils and that no fibril aggregation occurs. Therefore, it is considered that the APC fibrils are finely dispersed within the PMMA resin.

Fig. 4. Optical transparencies of neat PMMA and APC/PMMA nanocomposites containing 0.5, 1.0, and 2.0 wt% APC 2. All samples are around 0.5 mm thick.

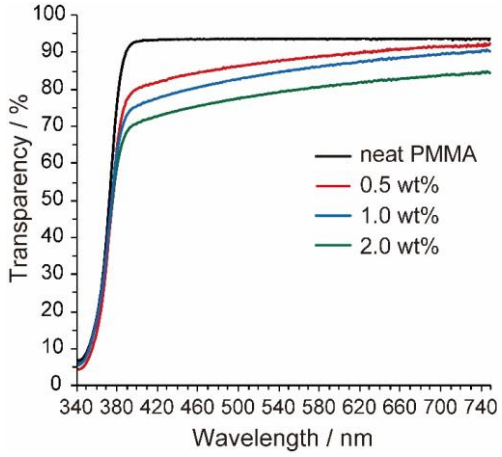

Fig. 5. Transparencies of PMMA and APC/PMMA nanocomposites [5].

3.4 Mechanical properties of the nanocomposites

The tensile properties of PMMA and nanocomposites are summarized in Table 2. The Young's moduli of the nanocomposites containing 0.5 and 1.0 wt% APC 2 are 82% and 155% higher than that of PMMA, respectively, indicating that APC serve as excellent reinforcements. The improvements in tensile properties achieved through the addition of APC are also confirmed by comparing the tensile strengths of the nanocomposites containing 0.5 and 1.0 wt% APC 2 with that of PMMA; the addition of 0.5 and 1.0 wt% APC improved the tensile strength of PMMA by 55% and 105%, respectively. On the other hand, the Young's modulus and strength of the nanocomposite containing 2.0 wt% APC was almost the same as that of PMMA. These results indicate that incorporating low amounts of APC (0.5 and 1.0 wt %) enhances tensile properties. On the other hand, high concentrations (2.0 wt%) of APC result in matrix embrittlement and the earlier onset of nanocomposite failure, which is also supported by the finding that the elongation at break of the 2.0 wt% sample was significantly lowered comparing with those of the 0.5 and 1.0 wt% samples.

Table 2. Tensile mechanical properties of PMMA and nanocomposites [5].

Sample	Tensile modulus/ GPa	Tensile strength / MPa	Elongation at break / %
PMMA	1.1	20	4.4
0.5 % APC/PMMA	2.0	31	3.0
1.0 % APC/PMMA	2.8	41	2.9
2.0 % APC/PMMA	1.2	19	2.2

The elongation at break of the composite decreases with denser reinforcing nanofibril network architecture; elongations at break of 3.0 % and 2.9 % were determined for the 0.5 and 1.0 wt% nanocomposites, respectively, while that of the 2.0 wt% composite was lower, at 2.2 %. On the other hand, PMMA showed a 4.4 % elongation at break. The lower elongations of the nanocomposites are related to the high APC surface area and strong interaction between amino groups of APC and acrylate groups of PMMA. Fig. 6 shows the expected intermolecular interactions between PMMA molecule and aminopropyl group on the APC surface: the acrylic group of PMMA has extremely strong adhesion because the amino group can form up to three hydrogen bonds [7], while the NFBC of APC has strong crystallinity and different mobility from the PMMA molecular chain. Therefore, PMMA itself has polymeric properties that do not allow it to elongate, but when it is combined with the strong NFBC, the mobility of PMMA is constrained, causing a decrease in the elongation at break.

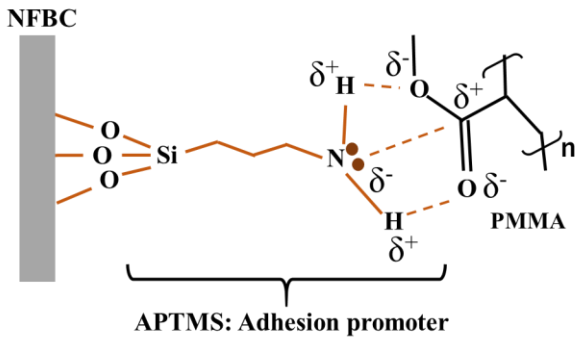

Fig. 6. Schematic illustration of interactions between APC surface and PMMA molecule.

The mechanical properties of the fiber-reinforced composites mainly depend on the properties of the used fibers such as tensile moduli and aspect ratio [8]. In this study, it was confirmed that the APC was uniformly dispersed in PMMA to form network structure and that the nanocomposites with high mechanical strengths could be obtained at low addition levels of APC. The improvement in the mechanical properties was due to the excellent features of NFBC. Therefore, the highly strong NFBC-enforced nanocomposite is expected to be applied as structural materials.

4. CONCLUSIONS

This study revealed that the surface of NFBC can be easily modified using APTMS in aqueous solution. Structural characterization and morphological observation of a series of APC samples prepared by controlling the APTMS-to-NFBC ratio revealed that characteristics of APC samples can be controlled by the feed amount of APTMS. The obtained APC is compatible with PMMA, and the composites prepared from PMMA and APC are highly transparent. In addition, the tensile strength of the composite obtained by adding only 1.0 wt% APC to PMMA was at least twice that of PMMA. Therefore, it is concluded that the surface-modified NFBC is suitable for an eco-friendly filler for fiber-reinforced resins that enhance physical properties.

ACKNOWLEDGMENTS

I would like to thank Prof. and Dr. Kenji Tajima and Dr. Tokuo Matsushima for collaboration on the early stages of this work. This work was supported in part by the Japan Society for the Promotion of Science (JSPS) [Grant No. JP21K05175 (H.K.)].

REFERENCES

[1] S. R. Djafari Petroudy, B. Chabot, E. Loranger, M. Naebe, J. Shojaeiarani, S. Gharehkhani, B. Ahvazi, J. Hu, and S. Thomas, *Energies*, **14,** 6792 (2021).
[2] K. Tajima, R. Kusumoto, R. Kose, H. Kono, T. Matsushima, T. Isono, T. Yamamoto, and T. Satoh, *Biomacromolecules*, **18,** 3432–3438 (2017).
[3] K. Tajima, K. Tahara, J. Ohba, R. Kusumoto, R. Kose, H. Kono, T. Matsushima, K. Fushimi, T. Isono, T. Yamamoto, and T. Satoh, *Biomacromolecules*, **21,** 581–588 (2020).
[4] H. Kono, T. Uno, H. Tsujisaki, H. Anai, R. Kishimoto, T. Matsushima, and K. Tajima, *ACS Appl. Nano Mater.*, **3,** 8232–8241 (2020).
[5] H. Kono, T. Uno, H. Tsujisaki, T. Matsushima, and K. Tajima, *ACS Omega*, **5,** 29561–29569 (2020).
[6] Y. Xie, C. A. S. Hill, Z. Xiao, H. Militz, and C. Mai, *Compos. Part A Appl. Sci. Manuf.*, **41,** 806–819 (2010).
[7] P. Chaijareenont, H. Takahashi, N. Nishiyama, M. Arksornnukit, *Dent. Mater. J.*, **31,** 610–616 (2012).
[8] C. Elanchezhian, B.Vijaya Ramnath, G. Ramakrishnan, M. Rajendrakumar, V. Naveenkumar, M. K. Saravanakumar, *Mater. Today: Proc.*, **5,** 1785–1790 (2018).